



UNIVERSITY OF
CAMBRIDGE

Department of Engineering

Inferring community characteristics in labelled networks

Author Name: Lawrence Tray

Supervisor: Ioannis Kontoyiannis

Date: 02/06/21

I hereby declare that, except where specifically indicated, the work submitted herein is my own original work.

Signed: _____ *Lawrence Tray* _____ *date:* _____ *02/06/21* _____

Technical Abstract

Labelled networks form a very common and important class of data, naturally appearing in numerous applications in science and engineering. A typical inference goal is to determine how the vertex labels (called features) affect the network’s graph structure. A standard approach has been to partition the network into blocks grouped by distinct values of the feature of interest. A block-based random graph model – typically a variant of the stochastic block model (SBM) – is then used to test for evidence of asymmetric behaviour within these feature-based communities. Nevertheless, the resulting communities often do not produce a natural partition of the graph. In this work we introduce a new generative model, the feature-first block model (FFBM), which is more effective at describing vertex-labelled undirected graphs and also facilitates the use of richer queries on labelled networks. We develop a Bayesian framework for inference with this model, and we present a method to efficiently sample from the posterior distribution of the FFBM parameters. The FFBM’s structure is kept deliberately simple to retain easy interpretability of the parameter values. We apply the proposed methods to a variety of network data to extract the most important features along which the vertices are partitioned. The main advantages of the proposed approach are that the whole feature-space is used automatically, and features can be rank-ordered implicitly according to impact. Any features that do not significantly impact the high-level structure can be discarded to reduce the problem dimension. In cases where the vertex features available do not readily explain the community structure in the resulting network, the approach detects this and is protected against over-fitting. Results on several real-world datasets illustrate the performance of the proposed methods.

Nomenclature

We provide a list of frequently used symbols for reference.

Table 1: Nomenclature

Symbol	Meaning
α	MH acceptance probability
π	MCMC target probability
ϕ	Softmax activation function
ψ	SBM parameters excluding b
θ	Feature-to-block generator parameters
ξ	Injected noise term in MALA
A	Graph adjacency matrix
b	Block membership vector
B	Total number of blocks
c	Dimensionality reduction cutoff
D	Feature-space dimension
e	Inter-block edge count matrix
E	Total number of edges
f	Fraction of vertices kept for training set
k	Degree sequence or standard deviation multiplier
\mathcal{L}	Average cross-entropy loss
N	Number of nodes in graph
q	MH proposal distribution
S	SBM description length
T	Length of Markov chain
\mathcal{T}	Retained sample set
U	Negative log-posterior for θ
w	Softmax weight vector
x	Feature vector
X	Feature matrix
y	Block membership posterior

Contents

1	Introduction	5
2	Preliminaries	6
3	Feature-first block model	6
3.1	Prior selection	7
4	Inference	8
4.1	Sampling block memberships	9
4.2	Sampling feature-to-block generator parameters	10
4.3	Sampling sequence	11
4.4	Dimensionality reduction	12
5	Experiments	13
5.1	Political books	15
5.2	Primary school dynamic contacts	16
5.3	Facebook egonet	16
6	Conclusion	17
A	Appendix: Additional material	22
A.1	SBM likelihood and prior	22
A.2	Choosing the MALA step-size	23
A.3	Burn-in and thinning	25
A.4	Initializing the b-chain	27
A.5	Dimensionality discussion	27
B	Appendix: Derivations	29
B.1	Derivation of conditional block distribution given feature matrix	29
B.2	Derivation of U form	29
B.3	Derivation of U gradient with respect to feature parameters	30
C	Appendix: Implementation details	32
C.1	Algorithms	32
C.2	Hyperparameter values	35
C.3	Hardware specification	35

D Risk assessment retrospective	36
E Covid-19 disruption	36

1 Introduction

A somewhat surprising property of many real-world networks is that they exhibit strong community structure; most nodes often belong to a densely connected cluster. There is high interest in recovering the latent communities from the observed graphs. The inferred communities can be exploited for compression algorithms [1] or used for link prediction in incomplete networks [11] to name a few applications.

We restrict our analysis to vertex-labelled networks. We shall refer to the vertex-labels as features. A common goal is to determine whether a given feature impacts graphical structure. To answer this from a Bayesian perspective we must use a random graph model; the standard is the stochastic block model (SBM) [21]. This is a latent variable model where each vertex belongs to a single block and the probability two nodes are connected depends only on the block memberships of each. There have been many variants to this model – the most popular being the mixed-membership stochastic block model (MMSBM) [7] and the overlapping stochastic block model (OSBM) [38]. Effectively, these just extend the model to allow each vertex to belong to multiple blocks simultaneously. However, a major drawback of these graphical models as applied to labelled networks is that they do not automatically include vertex features in the random graph generation process. Approaches based on graph neural networks [19] that utilise vertex features have been developed but these lack the easy interpretability of the simpler models.

To analyse a labelled network using one of the simple SBM variants, a typical inference procedure would be to partition the graph into blocks grouped by distinct values of the feature of interest. The associated model can then be used to test for evidence of heterogeneous connectivity between the feature-grouped blocks. Nevertheless, this approach is limited in that it can only consider one feature at a time. This makes it difficult to rank order the features by magnitude of impact. Lastly, the feature-grouped blocks are often an unnatural partition of the graph, leading to a poor model fit. We would instead prefer to partition the graph into its most natural blocks and then find which of the available features – if any – best predict the resulting partition.

With these desiderata in mind, we present a novel framework for modelling labelled networks, which we call the feature-first block model (FFBM). This is an extension of the SBM to labelled networks. We go on to present an efficient algorithm for sampling from the parameters of the feature-to-block generator. We can interpret the sampled FFBM parameters to determine which features have the largest impact on overall graphical structure.

2 Preliminaries

We first need a model for community-like structure in a network. For this we adopt the stochastic block model (SBM) - widely used across academia. Each node in the graph belongs to a unique community called a block. The probability that two nodes are connected depends only on the block memberships of each. Specifically, we will use the microcanonical variant of the SBM, proposed by Peixoto [27]. To allow for degree-variability between members of the same block, we must choose the degree-corrected formulation (DC-SBM).

Definition 2.1 (Microcanonical DC-SBM) *Let $N \in \mathbb{Z}^+$ denote the number of vertices in an undirected graph. The block memberships are encoded by a vector $b \in [B]^N$,¹ where $B \in \mathbb{Z}^+$ is the number of non-empty blocks. Let $e \in (\mathbb{Z}_0^+)^{N \times N}$ be the matrix of edge counts between blocks. e_{rs} is then the number of edges from block r onto block s – or twice that number if $r = s$. For undirected graphs, e is symmetric. Let $k \in (\mathbb{Z}_0^+)^N$ be a vector denoting the degree sequence of the graph. k_i is then the degree of vertex i . The graph’s adjacency matrix $A \in \{0, 1\}^{N \times N}$ is generated as follows:*

$$A \sim DC\text{-}SBM_{MC}(b, e, k) \quad (1)$$

Where edges are placed uniformly at random but respecting the constraints imposed by e , b and k – hence the microcanonical moniker. Specifically, A must satisfy the following:

$$e_{rs} = \sum_{i,j \in [N]} A_{ij} \mathbb{1}\{b_i = r\} \mathbb{1}\{b_j = s\} \quad \forall r, s \in [B] \quad \text{and} \quad k_i = \sum_{j \in [N]} A_{ij} \quad \forall i \in [N] \quad (2)$$

3 Feature-first block model

In this section we propose a novel generative model for labelled networks. We call this the feature-first block model (FFBM) and outline its structure in 1 As before, we let N denote the number of nodes and B the number of blocks in our graph. We define the vector $x_i \in \mathcal{X}^D$ as the feature vector for the i ’th vertex. D is the number of features. For the datasets we analyse, we deal with binary feature flags so $\mathcal{X} = \{0, 1\}$. The feature vectors $\{x_i\}_{i=1}^N$ may be compactly subsumed into the feature matrix $X \in \mathcal{X}^{N \times D}$.

For the FFBM, we start with the feature matrix X and probabilistically generate a vector of block memberships $b \in [B]^N$. The parameters of this step are encapsulated by θ . Each feature vector x_i is treated independently and used to generate the corresponding block

¹We introduce the notation $[K] := \{1, 2 \dots K\}$ to compactly define a set of K indices. Clearly, $[K]$ is only defined for $K \in \mathbb{Z}^+$.

membership $b_i \in [B]$. We choose a single softmax layer to model $p(b_i|x_i, \theta)$. More complex models are possible but then deriving meaning from the inferred parameter distributions is more difficult. Summarising, we write $p(b|X, \theta)$ as follows:

$$p(b|X, \theta) = \prod_{i=1}^N p(b_i|x_i, \theta) = \prod_{i=1}^N \phi_{b_i}(x_i; \theta) = \prod_{i=1}^N \frac{\exp(w_{b_i}^T x_i)}{\sum_{k=1}^B \exp(w_k^T x_i)} \quad (3)$$

We deliberately exclude a bias term to ensure that the relationships we model are based on features and not information about the size of each detected block; a more complete discussion on this topic is given in A.5. The parameter vector θ for this stage contains all the weight vectors $\theta = \{w_k\}_{k=1}^B$. Each w_k has dimension D . We could instead write the parameters θ as a $B \times D$ matrix of weights W ; this form has computational benefits as then $z_i := Wx_i$, which is the input to the softmax activation function.

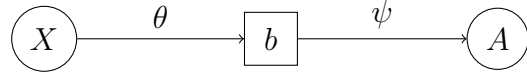


Figure 1: The feature-first block model (FFBM)

Once the block memberships b have been generated, we then draw the graph A from the microcanonical DC-SBM (equation 4) with additional parameters encapsulated by $\psi = \{\psi_e, \psi_k\}$.

$$A \sim \text{DC-SBM}_{\text{MC}}(b, \psi_e, \psi_k) \quad (4)$$

3.1 Prior selection

Before performing any inference, we must specify priors on θ and ψ . For θ it seems sensible to choose a Gaussian prior, with zero mean and variance matrix $\sigma_\theta^2 I$ such that each element of θ is independent and distributed like $\sim \mathcal{N}(0, \sigma_\theta^2)$. In vector form, the prior for θ is therefore:

$$p(\theta) = \mathcal{N}(\theta; 0, \sigma_\theta^2 I) \quad (5)$$

In our model, the block memberships vector b is an intermediate latent variable and so we are not free to choose a prior for it. Nevertheless, as far as inference on the right-hand-side of figure 1, we regard $p(b|X)$ as a pseudo-prior on b . We can show (appendix B.1) that our choice of prior for $p(\theta)$ in equation 5 leads to a uniform $p(b|X)$ in equation 6.

$$p(b|X) = \int p(b|X, \theta)p(\theta)d\theta = B^{-N} \quad (6)$$

This is an enormously important simplification as evaluating $p(b|X)$ does not require an expensive Monte-Carlo integration over the θ -domain nor does it require the exact value of X . Peixoto [27] proposes careful choices for the additional microcanonical SBM parameters ψ which we adopt. Peixoto's idea is to write the joint prior on (b, e, k) as a product of conditionals $p(b, e, k) = p(b)p(e|b)p(k|e, b) = p(b)p(\psi|b)$. For our purposes we must insert a conditioning on X , to form our pseudo-prior for b and ψ , to give equation 7.

$$p(b, \psi|X) = p(b|X)p(\psi|b, X) = p(b|X)p(\psi|b) \quad (7)$$

Where we leverage the fact $(\psi \perp\!\!\!\perp X)|b$. We then borrow the priors proposed by Peixoto [27] for $p(\psi|b)$ to complete our model. Please refer to appendix A.1 for the exact form of $p(\psi|b)$. All that concerns the main argument is we have a computable form.

4 Inference

Now that we have defined the FFBM, we wish to leverage it to perform inference. Suppose we are presented with a vertex-labelled graph (A, X) ; the goal is to draw samples for θ according to the posterior given the observed data:

$$\theta^{(t)} \sim p(\theta|A, X) \quad (8)$$

However, generating these samples is not easily done in practice. We therefore propose an iterative approach. We first draw samples $b^{(t)}$ from the block membership posterior (equation 9) and then use each $b^{(t)}$ to draw samples for θ as in equation 10.

$$b^{(t)} \sim p(b|A, X) \quad (9)$$

$$\theta^{(t)} \sim p(\theta|X, b^{(t)}) \quad (10)$$

Both of these sampling steps can be implemented with a Markov Chain through the Metropolis-Hastings algorithm [13]. We just need to define a proposal distribution $q(x, x')$ for proposing a move $x \rightarrow x'$ and be able to evaluate an un-normalised form of the target distribution, denoted $\pi(\cdot)$, point-wise. The proposed move is then accepted with probability α (equation 11) else it is rejected and we stay at x .

$$\alpha(x, x') = \min \left(\frac{\pi(x')q(x', x)}{\pi(x)q(x, x')}, 1 \right) \quad (11)$$

This accept-reject step ensures the resulting Markov Chain is in detailed balance with the target distribution $\pi(\cdot)$. What we propose in equations 9 and 10 is therefore implemented through a 2-level Markov chain. The resulting samples for $\theta^{(t)}$ are unbiased in the sense that the expectation of their distribution is the posterior we are targetting:

$$\mathbb{E}_{b^{(t)}} [p(\theta|X, b^{(t)})] = \sum_{b \in [B]^N} p(\theta|X, b)p(b|A, X) = \sum_{b \in [B]^N} p(\theta, b|A, X) = p(\theta|A, X) \quad (12)$$

This is an example of a pseudo-marginal approach. Indeed, Andrieu and Roberts [8] show that the unbiased result in equation 12 is sufficient to prove that for large enough t , $\theta^{(t)} \sim \mathbb{E}_{b^{(t)}} [p(\theta|X, b^{(t)})] = p(\theta|A, X)$ which is exactly the distribution we are targetting (equation 8).

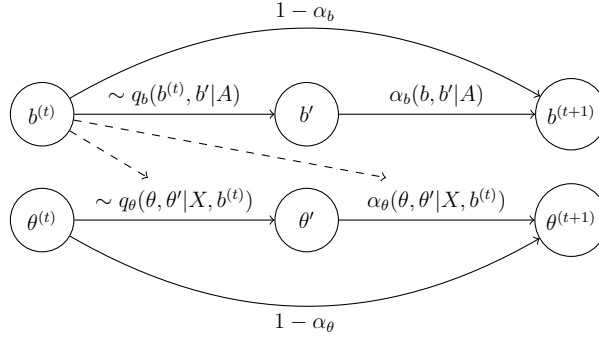


Figure 2: Sampling sequence

The reason we split the Markov chain into two stages is because the summation over all latent states $b \in [B]^N$ required to directly compute the likelihood $p(A|X, \theta) = \sum_{b \in [B]^N} p(A|b)P(b|X, \theta)$ is intractable – $O(B^N)$. Figure 2 shows an overview of the proposed method. We have introduced subscripts and conditionings to make explicit what variables each step utilises. We note the power of the simplification given by equation 6. As $p(b|X)$ does not depend on the exact value of X , we do not need to know the value of X to perform the sampling on b . Conversely, for the $\theta^{(t)}$ samples, we use only $b^{(t)}$ but not A as $(\theta \perp\!\!\!\perp A)|b$.

4.1 Sampling block memberships

Peixoto [25] proposes a Monte Carlo method which we will base our approach on. It relies on writing the posterior in the following form:

$$p(b|A, X) \propto p(A|b, X) \cdot p(b|X) = \pi_b(b) \quad (13)$$

Now $\pi_b(\cdot)$ is the un-normalised density we wish to sample from for the b -chain. In other

words, we wish to construct a Markov chain that has $\pi_b(\cdot)$ as its invariant distribution. We can break π_b down as follows:

$$\pi_b(b) = p(b|X) \sum_{\psi} p(A, \psi|b, X) = p(b|X)p(A, \psi^*|b, X) = p(A|b, \psi^*) \cdot p(\psi^*|b) \cdot p(b|X) \quad (14)$$

Since we are using the microcanonical SBM formulation, there is only one value of ψ that is compatible with the given (A, b) pair (given in equation 2). We denote this value $\psi^* = \{\psi_k^*, \psi_e^*\}$. Therefore, the summation over all ψ reduces to just the single ψ^* term; this is the power of the microcanonical formulation. We also define the microcanonical entropy of the configuration as.

$$S(b) = -\log \pi_b(b) = -\left(\log p(A|b, \psi^*) + \log p(\psi^*, b|X) \right) \quad (15)$$

This entropy can equally be thought of as the description length of the graph. The exact form of the proposal q_b is explored thoroughly by Peixoto [25] and not repeated here. There is a widely used library for Python made available under LGPL called `graph-tool` [26], which implements this algorithm. The only modification we make is in the block membership prior $p(b)$ which we replace with $p(b|X) = B^{-N}$, which cancels out in the MH accept-reject step as it is independent of b .

4.2 Sampling feature-to-block generator parameters

The invariant distribution we wish to target for the θ samples is the posterior of θ given the values of the pair (X, b) . We write this as follows:

$$\pi_\theta(\theta) \propto p(\theta|X, b) \propto p(b|X, \theta)p(\theta) \propto \pi_\theta(\theta) \propto \exp(-U(\theta)) \quad (16)$$

Where we have introduced $U(\theta)$ equal to the negative log posterior. We define $y_{ij} := \mathbb{1}\{b_i = j\}$ and $a_{ij} := \phi_j(x_i; \theta)$. Discarding constant terms, we can write $U(\theta)$ as in equation 17 (refer to appendix B.2 for the derivation).

$$U(\theta) = \left(\sum_{i=1}^N \sum_{j=1}^B y_{ij} \log \frac{1}{a_{ij}} \right) + \frac{1}{2\sigma_\theta^2} \|\theta\|^2 = N \cdot \mathcal{L}(\theta) + \frac{1}{2\sigma_\theta^2} \|\theta\|^2 \quad (17)$$

$U(\theta)$ in equation 17 appears a typical objective function for neural network training. The first term is introduced by the likelihood. We collect it into $N \cdot \mathcal{L}(\theta)$, which is the cross-entropy between the graph-predicted and feature-predicted block memberships summed over all vertices. The second term of equation 17 – introduced by the prior – brings a form of

regularisation, guarding against over-fitting. Different to traditional applications, our goal is not to find the minimiser of $U(\theta)$ but to draw samples from the posterior $\pi_\theta(\cdot) \propto \exp(-U(\cdot))$. We can use ∇U as a useful heuristic to bias our proposal towards regions of higher target density. We therefore adopt the Metropolis-adjusted Langevin algorithm (MALA) – first proposed by Roberts and Tweedie [29]. Given the current sample θ , we generate a new sample θ' according to equation 18.

$$\theta' = \theta - h \nabla U(\theta) + \sqrt{2h} \cdot \xi \quad (18)$$

$$\therefore q_\theta(\theta, \theta') = \mathcal{N}(\theta'; \theta - h \nabla U(\theta), 2hI) \quad (19)$$

Where $\xi \sim \mathcal{N}(0, I)$ and h is a step-size parameter – which may vary with the sample index (appendix A.2 explores this more fully). Without the injected noise term, MALA is equivalent to gradient descent. We require the noise term ξ to fully explore the parameter space. We can write the proposal distribution q_θ as in equation 19. The term ∇U has an easy to compute analytic form (derived in Appendix B.3). By noting that $\theta = \{w_k\}_{k=1}^B$, we write the derivative with respect to each w_k as:

$$\frac{\partial U}{\partial w_k} = - \left(\sum_{i=1}^N \left\{ \tilde{x}_i(y_{ik} - a_{ik}) \right\} - \frac{w_k}{\sigma_\theta^2} \right) \quad (20)$$

After a proposed move is generated, in typical Metropolis-Hastings fashion we accept the move with probability α_θ , as in equation 11.

4.3 Sampling sequence

Up to this point, each $\theta^{(t)}$ update uses its corresponding $b^{(t)}$ sample. This means that the evaluation of $U(\theta)$ and $\nabla U(\theta)$ has high variance. This may lead to longer burn-in for the resulting Markov chain. The only link between $b^{(t)}$ and $\theta^{(t)}$ is in the evaluation of $U(\theta)$ and $\nabla U(\theta)$ which depends only on the matrix $y^{(t)}$ with entries $y_{ij}^{(t)} := \mathbb{1}\{b_i^{(t)} = j\}$. We would rather deal with the expectation of each $y_{ij}^{(t)}$:

$$\mathbb{E} \left[y_{ij}^{(t)} \right] = \mathbb{E}_{b^{(t)}} \left[\mathbb{1}(b_i^{(t)} = j) \right] = p(b_i = j | A, X) \quad (21)$$

We can obtain an unbiased estimate for this quantity using the set of b -samples. However, as with all MCMC methods, we must only use samples after burn-in and thinning have been applied. We introduce \mathcal{T}_b to denote the retained set of indices for the b -samples and \mathcal{T}_θ similarly for the θ -chain. An in-depth discussion of how these sets are chosen is given in

appendix A.3. The unbiased estimate for $y_{ij}^{(t)}$ using the restricted sample set \mathcal{T}_b is denoted \hat{y}_{ij} and has form:

$$\hat{y}_{ij} := \frac{1}{|\mathcal{T}_b|} \sum_{t \in \mathcal{T}_b} y_{ij}^{(t)} = \frac{1}{|\mathcal{T}_b|} \sum_{t \in \mathcal{T}_b} \mathbb{1}\{b_i^{(t)} = j\} \quad (22)$$

We choose to feed each $\theta^{(t)}$ update step the same matrix \hat{y} for all t rather than the corresponding $y^{(t)}$. This means we no longer need to run the b and θ Markov chains concurrently. Instead, we run the b -chain to completion and use it to generate \hat{y} . This affords us the flexibility to vary the lengths of the b and θ -chains. Furthermore, the changeover from $y^{(t)}$ to \hat{y} reduces the burn-in time for the θ -chain by reducing the variance in our evaluation of U and ∇U . A description of the overall algorithms is given in appendix C.1.

4.4 Dimensionality reduction

Once we have the samples $\{\theta^{(t)}\} \sim p(\theta|A, X)$, we can compute the empirical mean and standard deviation of each component of θ . Switching back to matrix notation we define $\theta = W$, such that W_{ij} is the weight component for block i and feature j , we can define:

$$\hat{\mu}_{ij} := \frac{1}{|\mathcal{T}_\theta|} \sum_{t \in \mathcal{T}_\theta} W_{ij}^{(t)} \quad \text{and} \quad \hat{\sigma}_{ij} := \frac{1}{|\mathcal{T}_\theta|} \sum_{t \in \mathcal{T}_\theta} \left(W_{ij}^{(t)} - \hat{\mu}_{ij} \right)^2 \quad (23)$$

A simple heuristic to discard the least important features requires specifying a cutoff $c > 0$ and a multiplier $k > 0$. We define the function $\mathcal{F}_i(j)$ as in 24 then only keep features with indices $d \in \mathcal{D}'$, where \mathcal{D}' is constructed as in equation 25.

$$\mathcal{F}_i(j) := (\hat{\mu}_{ij} - k\hat{\sigma}_{ij}, \hat{\mu}_{ij} + k\hat{\sigma}_{ij}) \cap (-c, +c) \quad (24)$$

$$\mathcal{D}' := \{j \in [D] : \exists i \in [B] \text{ s.t. } \mathcal{F}_i(j) \neq \emptyset\} \quad (25)$$

Intuitively, this means discarding any feature for which $\hat{\mu}_{ij} \pm k\hat{\sigma}_{ij}$ lies within or spans the null region $(-c, c)$ for all block indices. If we were to use the Laplace approximation for the posterior $p(W_{ij}|A, X) \approx \mathcal{N}(W_{ij}; \mu_{ij}, \sigma_{ij})$, then this is effectively a hypothesis test on the value of W_{ij} (equation 26). \mathcal{D}' then comprises all features i for which H_1 is accepted at least once for some $j \in [B]$.

$$H_0 : |W_{ij}| \leq c \quad H_1 : |W_{ij}| > c \quad (26)$$

The multiplier k determines the degree of significance of the result. However, as the Laplace approximation is not exact we will only treat this dimensionality reduction method as a useful heuristic and not an exact method. Conversely, we could fix $k = k_0$ and the dimension of our reduced feature set $|\mathcal{D}'| = D'$. We would then like to find the largest value of c such

that $|\mathcal{D}'| = D'$ given $k = k_0$. This is summarised in equation 27. This approach is often preferred as it fixes the number of reduced dimensions.

$$c^* = \arg \max_{c>0} (c : |\mathcal{D}'| = D', k = k_0) \quad (27)$$

For an algorithmic implementation of this method refer to appendix C.1.

5 Experiments

We apply the developed methods to a variety of datasets. These are chosen to span a range of node counts N , edge counts E and feature space dimension D . We consider the following:

- **Political books** [22] ($N = 105, E = 441, D = 3$) – network of Amazon book sales about U.S. politics, published close to the presidential election in 2004. Two books are connected if they were frequently co-purchased by customers. Vertex features encode the political affiliation of the author (liberal, conservative or neutral).
- **Primary school dynamic contacts** [33] ($N = 238, E = 5539, D = 13$) – network of face-to-face contacts amongst students and teachers at a primary school in Lyon, France. Two nodes are connected if the two parties shared a face-to-face interaction over the school-day. Vertex features include class membership (one of 10 values: 1A-5B), gender (male, female) and teacher status encoded as an 11th school-class. No further identifiable information is retained. We choose to analyse just the second day of results.
- **Facebook egonet** [16] ($N = 747, E = 30025, D = 480$) – an assortment of Facebook users’ friends lists. Vertex features are extracted from each user’s profile and are fully anonymised. They include information about education history, languages spoken, gender, home-town, birthday etc. We focus on the egonet with id 1912.

Table 2: Experimental results averaged over $n = 10$ iterations (mean \pm standard deviation)

Dataset	B	D	D'	\bar{S}_e	$\bar{\mathcal{L}}_0$	$\bar{\mathcal{L}}_1$	c^*	$\bar{\mathcal{L}}'_0$	$\bar{\mathcal{L}}'_1$
Polbooks	3	3	–	2.250 ± 0.000	0.563 ± 0.042	0.595 ± 0.089	–	–	–
School	10	13	10	1.894 ± 0.004	0.787 ± 0.127	0.885 ± 0.129	1.198 ± 0.249	0.793 ± 0.132	0.853 ± 0.132
FB egonet	10	480	10	1.626 ± 0.003	1.326 ± 0.043	1.538 ± 0.069	0.94 ± 0.019	1.580 ± 0.150	1.605 ± 0.106

We require metrics to assess performance. This can be split into two separate components: the microcanonical SBM fit (concerned with the b -samples) and the fit of the feature-to-block generator (concerned with the θ -samples). Starting with the SBM, $S(b)$ (equation 15) can be interpreted as the description length of the partition imposed by b . It is only natural to

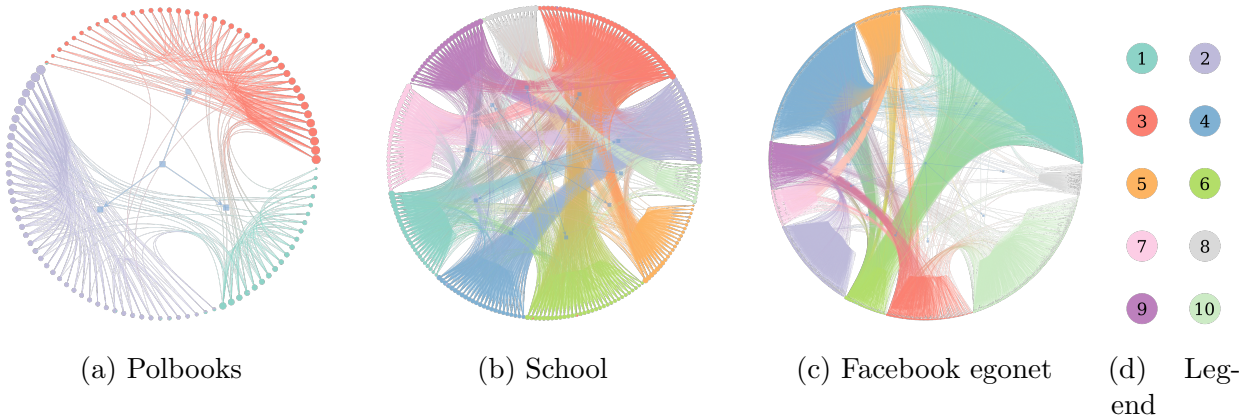


Figure 3: Networks laid out and coloured according by inferred block memberships \hat{y} for a given experiment iteration. Visualisation performed using *graph-tool* [26]

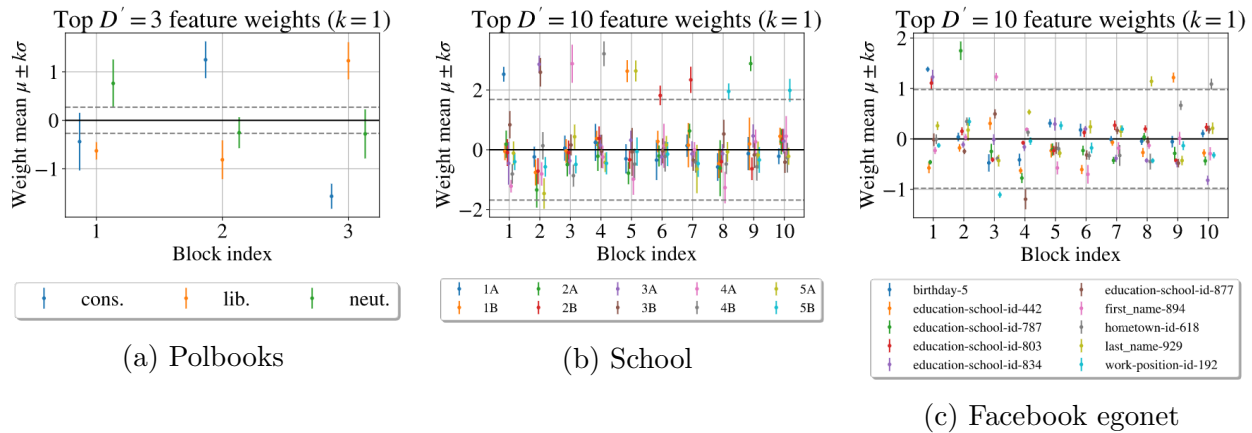


Figure 4: Reduced dimension feature-to-block generator weight samples

divide this quantity by the number of entities (nodes and edges) in our graph $N + E$ to allow for rough comparison between graphs. This defines a simple metric to gauge the fit of the SBM: the description length per entity averaged over the b -samples (equation 28):

$$\bar{S}_e := \frac{1}{(N+E)|\mathcal{T}_b|} \sum_{t \in \mathcal{T}_b} S(b^{(t)}) \quad (28)$$

However, to assess the performance of the feature-to-block predictor, we must partition the vertex set $[N]$ into training and test sets. We choose to randomly partition the vertices on each experiment run such that a constant fraction f of the available vertices go to form our training set \mathcal{G}_0 and the remainder are held out to form our test set \mathcal{G}_1 . The b -chain is run using the whole network but we only use vertices $v \in \mathcal{G}_0$ to train the θ -chain. As $|\mathcal{G}_0| \neq |\mathcal{G}_1|$ in general, we cannot use the un-normalised log target U (equation 17) for comparison as the

total cross-entropy loss is scaled by the size of each set but the prior term stays constant. We therefore must use the average cross-entropy loss over each set (equation 29):

$$\bar{\mathcal{L}}_\star := \frac{1}{|\mathcal{T}_\theta|} \sum_{t \in \mathcal{T}_\theta} \mathcal{L}_\star(\theta^{(t)}) \quad \text{where} \quad \mathcal{L}_\star(\theta^{(t)}) := \frac{1}{|\mathcal{G}_\star|} \sum_{i \in \mathcal{G}_\star} \sum_{j \in [B]} \hat{y}_{ij} \log \frac{1}{\phi_j(x_i; \theta^{(t)})} \quad (29)$$

Where $\star \in \{0, 1\}$ has been introduced to toggle between training and test sets. Table 2 summarises the results for each experiment.² We also apply the dimensionality reduction method on the two higher dimensional datasets (the school and FB egonet). For this we leverage equation 27, to reduce the dimension from D to D' with $k = 1$ to yield the maximal cutoff c^* . We then retrain the feature-block predictor using just the retained feature set \mathcal{D}' and report the loss over the training and test sets for the reduced classifier – denoted $\bar{\mathcal{L}}'_0$ and $\bar{\mathcal{L}}'_1$ respectively. These values are also included in table 2.

Table 2 already highlights some general trends in the results. Firstly, the variance of the test loss $\bar{\mathcal{L}}_1$ tends to be higher than the training loss $\bar{\mathcal{L}}_0$. This is expected as our test set is smaller than the training set and so more susceptible to variability in its construction. Indeed, most of the variance in the evaluation of $\bar{\mathcal{L}}_0$ and $\bar{\mathcal{L}}_1$ comes from the random partitioning of the graph into training and test sets. Secondly, it can be seen that the dimensionality reduction procedure brings the training and test losses closer together. This implies that the features we keep are indeed correlated with the underlying graphical partition and that the approach generalises correctly.

The average description length per entity of the graph \bar{S}_e has very low variance implying the detected communities can be found reliably (to within an arbitrary relabelling of blocks). For reference we plot an inferred partition for each of the graphs on figure 3. The polbooks graph yields the cleanest separation between blocks but nonetheless the inferred partitions for the other datasets do succeed at partitioning the graph into densely connected clusters.

5.1 Political books

We wish to determine whether the author’s political affiliation is a good predictor of the overall network structure. We choose to partition the network into $B = 3$ communities as we only have this many distinct values for political affiliation (conservative, liberal or neutral). From, figure 4a, we see that all 3 blocks have a distinct political affiliation as their largest positive component. This is strong evidence that political affiliation is indeed the axis which best predicts the 3-way natural partition of the graph into blocks. Furthermore, from table 2 we see that the training and test losses are very similar and both are low in magnitude.

²For a comprehensive list of the hyper-parameters used for each experiment please see appendix C.2

This provides further evidence to the claim that political affiliation is the best explanatory variable for the overall network structure.

5.2 Primary school dynamic contacts

We choose $B = 10$ in line with the total number of school-classes. As before, we sample the block-generator parameters θ and employ the dimensionality reduction technique with standard deviation multiplier $k = 1$ to pick out the top $D' = 10$ features. We then plot the weights for the surviving features $d \in \mathcal{D}'$ on figure 4b. Immediately, we see that only the pupils' class memberships have survived (1A-5B); gender and teacher/student status have been discarded meaning that these are not good predictors of overall macro-structure.

The vast majority of blocks are composed of a single class. However, some blocks have 2 comparably good classes as their predictor. For example, block 2 contains classes 3A and 3B as its 2 best predictors. This suggests that the social divide between classes is less pronounced for pupils in year 3. Conversely, some classes are found to extend over two detected blocks (class 2B spans blocks 6 and 7) but we nonetheless do not have a feature which explains the division. The most surprising block is number 5 - which has comparable weightings for classes 5A and 1B. Perhaps there was a joint event between those two classes on the day the data were collected.

5.3 Facebook egonet

We choose $B = 10$ and $D' = 10$ for this experiment. The remaining features (figure 4c) are those that best explain the high-level community structure. The majority of the surviving features are education related. Nevertheless, for $D' = 10$ we only have good explanations for the makeup of some of the detected blocks; several blocks in figure 4c do not have high-magnitude components for $D' = 10$.

When the feature dimension is very large, it becomes increasingly likely that a particular feature may uniquely identify a small set of nodes. If these nodes are all part of the same community then the classifier will overfit for that particular parameter. The regularisation term imposed by the prior goes some way to alleviating this problem. Nevertheless, we see in figure 4c that the feature `birthday-5` has a very high weight as it relates to block 1 – but it would be preposterous to conclude that birthdays determine graphical structure. The analyst must remain vigilant of such problems.

6 Conclusion

The FFBM was developed to address the shortcomings of other graphical models when testing how vertex features affect community structure. The idea is to divide the graph into its most natural partition and test whether the vertex features can accurately explain this partition. It is very easy to find vertex features that are in some way correlated with the graphical structure. Nonetheless, only when we find the feature that best describes the most pronounced partition do we have a stronger case for causation.

With the newly-defined FFBM, we go on to present an efficient inference algorithm to sample the parameters θ of the feature-to-block generator. This is introduced as two concurrent Markov chains to sample the block memberships b and block generator parameters θ . Nevertheless, we can serialise the chains and use the empirical mean of the b -samples as the input to our θ -chain. This reduces the variance in our evaluation of the target distribution and thus shortens burn-in.

The overall method is shown to be effective at extracting and describing the most natural communities in a labelled network. Nevertheless, the approach can only currently explain the structure at the macro-scale. We cannot explain structure within each block. Future work will benefit from extending the FFBM to be hierarchical in nature. That way, the structure of the network can be explained at all length-scales of interest. So long as data collection techniques remain ethical and care is taken to respect personal privacy, such empowered decision-making can only help humankind.

References

- [1] Emmanuel Abbe. Graph compression: The effect of clusters. In *2016 54th Annual Allerton Conference on Communication, Control, and Computing (Allerton)*, pages 1–8, 2016. doi: 10.1109/ALLERTON.2016.7852203.
- [2] Emmanuel Abbe. Community detection and stochastic block models: Recent developments. *Journal of Machine Learning Research*, 18(177):1–86, 2018. URL <http://jmlr.org/papers/v18/16-480.html>.
- [3] Emmanuel Abbe and Colin Sandon. Recovering communities in the general stochastic block model without knowing the parameters. In C. Cortes, N. Lawrence, D. Lee, M. Sugiyama, and R. Garnett, editors, *Advances in Neural Information Processing Systems*, volume 28, pages 676–684. Curran Associates, Inc., 2015. URL <https://proceedings.neurips.cc/paper/2015/file/cfee398643cbc3dc5eefc89334cacdc1-Paper.pdf>.
- [4] Emmanuel Abbe and Colin Sandon. Achieving the k_s threshold in the general stochastic block model with linearized acyclic belief propagation. In D. Lee, M. Sugiyama, U. Luxburg, I. Guyon, and R. Garnett, editors, *Advances in Neural Information Processing Systems*, volume 29, pages 1334–1342. Curran Associates, Inc., 2016. URL <https://proceedings.neurips.cc/paper/2016/file/6c29793a140a811d0c45ce03c1c93a28-Paper.pdf>.
- [5] Emmanuel Abbe and Colin Sandon. Proof of the achievability conjectures for the general stochastic block model. *Communications on Pure and Applied Mathematics*, 71(7):1334–1406, 2018. doi: <https://doi.org/10.1002/cpa.21719>. URL <https://onlinelibrary.wiley.com/doi/abs/10.1002/cpa.21719>.
- [6] Lada A. Adamic and Natalie Glance. The political blogosphere and the 2004 us election. In *Proceedings of the WWW-2005 Workshop on the Weblogging Ecosystem*, 2005.
- [7] Edo M Airoldi, David Blei, Stephen Fienberg, and Eric Xing. Mixed membership stochastic blockmodels. In D. Koller, D. Schuurmans, Y. Bengio, and L. Bottou, editors, *Advances in Neural Information Processing Systems*, volume 21. Curran Associates, Inc., 2009. URL <https://proceedings.neurips.cc/paper/2008/file/8613985ec49eb8f757ae6439e879bb2a-Paper.pdf>.
- [8] Christophe Andrieu and Gareth O. Roberts. The pseudo-marginal approach for efficient

- Monte Carlo computations. *The Annals of Statistics*, 37(2):697 – 725, 2009. doi: 10.1214/07-AOS574. URL <https://doi.org/10.1214/07-AOS574>.
- [9] Jevin West et al. The role of gender in scholarly authorship. *PLoS One*, 2013.
 - [10] T S Evans. Clique graphs and overlapping communities. *Journal of Statistical Mechanics: Theory and Experiment*, 2010(12):P12037, Dec 2010. ISSN 1742-5468. doi: 10.1088/1742-5468/2010/12/p12037. URL <http://dx.doi.org/10.1088/1742-5468/2010/12/P12037>.
 - [11] Solenne Gaucher, Olga Klopp, and Geneviève Robin. Outliers detection in networks with missing links, 2020.
 - [12] Aric A. Hagberg, Daniel A. Schult, and Pieter J. Swart. Exploring network structure, dynamics, and function using networkx. In Gaël Varoquaux, Travis Vaught, and Jarrod Millman, editors, *Proceedings of the 7th Python in Science Conference*, pages 11 – 15, Pasadena, CA USA, 2008.
 - [13] W. K. Hastings. Monte carlo sampling methods using markov chains and their applications. *Biometrika*, 57(1):97–109, 1970. ISSN 00063444. URL <http://www.jstor.org/stable/2334940>.
 - [14] Matthew Kraatz, Nina Shah, and Emmanuel Lazega. The collegial phenomenon: The social mechanisms of cooperation among peers in a corporate law partnership. *Administrative Science Quarterly*, 48:525, 09 2003. doi: 10.2307/3556688.
 - [15] Jure Leskovec and Andrej Krevl. SNAP Datasets: Stanford large network dataset collection, June 2014. URL <http://snap.stanford.edu/data>.
 - [16] Jure Leskovec and Julian Mcauley. Learning to discover social circles in ego networks. In F. Pereira, C. J. C. Burges, L. Bottou, and K. Q. Weinberger, editors, *Advances in Neural Information Processing Systems*, volume 25. Curran Associates, Inc., 2012. URL <https://proceedings.neurips.cc/paper/2012/file/7a614fd06c325499f1680b9896beedeb-Paper.pdf>.
 - [17] Jure Leskovec and Rok Sosić. Snap: A general-purpose network analysis and graph-mining library. *ACM Transactions on Intelligent Systems and Technology (TIST)*, 8(1):1, 2016.
 - [18] Benjamin F. Maier and Dirk Brockmann. Cover time for random walks on arbitrary complex networks. *Phys. Rev. E*, 96:042307, Oct 2017. doi: 10.1103/PhysRevE.96.042307. URL <https://link.aps.org/doi/10.1103/PhysRevE.96.042307>.

- [19] Nikhil Mehta, Lawrence Carin Duke, and Piyush Rai. Stochastic blockmodels meet graph neural networks. In Kamalika Chaudhuri and Ruslan Salakhutdinov, editors, *Proceedings of the 36th International Conference on Machine Learning*, volume 97 of *Proceedings of Machine Learning Research*, pages 4466–4474. PMLR, 09–15 Jun 2019. URL <http://proceedings.mlr.press/v97/mehta19a.html>.
- [20] Christopher Nemeth and Paul Fearnhead. Stochastic gradient markov chain monte carlo. *Journal of the American Statistical Association*, 116(533):433–450, 2021. doi: 10.1080/01621459.2020.1847120. URL <https://doi.org/10.1080/01621459.2020.1847120>.
- [21] Krzysztof Nowicki and Tom A. B Snijders. Estimation and prediction for stochastic block-structures. *Journal of the American Statistical Association*, 96(455):1077–1087, 2001. doi: 10.1198/016214501753208735. URL <https://doi.org/10.1198/016214501753208735>.
- [22] Boris Pasternak and Ivor Ivask. Four unpublished letters. *Books Abroad*, 44(2):196–200, 1970. ISSN 00067431. URL <http://www.jstor.org/stable/40124305>.
- [23] Tiago P. Peixoto. Parsimonious module inference in large networks. *Phys. Rev. Lett.*, 110:148701, Apr 2013. doi: 10.1103/PhysRevLett.110.148701. URL <https://link.aps.org/doi/10.1103/PhysRevLett.110.148701>.
- [24] Tiago P. Peixoto. Parsimonious module inference in large networks. *Physical Review Letters*, 110(14), Apr 2013. ISSN 1079-7114. doi: 10.1103/physrevlett.110.148701. URL <http://dx.doi.org/10.1103/PhysRevLett.110.148701>.
- [25] Tiago P. Peixoto. Efficient monte carlo and greedy heuristic for the inference of stochastic block models. *Physical Review E*, 89(1), Jan 2014. ISSN 1550-2376. doi: 10.1103/physreve.89.012804. URL <http://dx.doi.org/10.1103/PhysRevE.89.012804>.
- [26] Tiago P. Peixoto. The graph-tool python library. *figshare*, 2014. doi: 10.6084/m9.figshare.1164194. URL http://figshare.com/articles/graph_tool/1164194.
- [27] Tiago P. Peixoto. Nonparametric bayesian inference of the microcanonical stochastic block model. *Physical Review E*, 95(1), Jan 2017. ISSN 2470-0053. doi: 10.1103/physreve.95.012317. URL <http://dx.doi.org/10.1103/PhysRevE.95.012317>.
- [28] Tiago P. Peixoto. Nonparametric weighted stochastic block models. *Physical Review E*, 97(1), Jan 2018. ISSN 2470-0053. doi: 10.1103/physreve.97.012306. URL <http://dx.doi.org/10.1103/PhysRevE.97.012306>.

- [29] Gareth O. Roberts and Richard L. Tweedie. Exponential convergence of Langevin distributions and their discrete approximations. *Bernoulli*, 2(4):341 – 363, 1996. doi: [bj/1178291835](https://doi.org/). URL <https://doi.org/>.
- [30] Benedek Rozemberczki, Carl Allen, and Rik Sarkar. Multi-scale attributed node embedding, 2019.
- [31] Benedek Rozemberczki, Carl Allen, and Rik Sarkar. Multi-scale attributed node embedding, 2019.
- [32] Yi Song and Stephane Bressan. Force-directed layout community detection. *School of Computing*, 2013.
- [33] Juliette Stehlé, Nicolas Voirin, Alain Barrat, Ciro Cattuto, Lorenzo Isella, Jean-François Pinton, Marco Quaggiotto, Wouter Van den Broeck, Corinne Régis, Bruno Lina, and Philippe Vanhems. High-resolution measurements of face-to-face contact patterns in a primary school. *PLOS ONE*, 6(8):1–13, 08 2011. doi: [10.1371/journal.pone.0023176](https://doi.org/10.1371/journal.pone.0023176). URL <https://doi.org/10.1371/journal.pone.0023176>.
- [34] Jie Tang, Jing Zhang, Limin Yao, Juanzi Li, Li Zhang, and Zhong Su. Arnetminer: Extraction and mining of academic social networks. In *KDD’08*, pages 990–998, 2008.
- [35] Max Welling and Yee Whye Teh. Bayesian learning via stochastic gradient langevin dynamics. In *Proceedings of the 28th International Conference on International Conference on Machine Learning*, ICML’11, page 681–688, Madison, WI, USA, 2011. Omnipress. ISBN 9781450306195.
- [36] T. Xifara, C. Sherlock, S. Livingstone, S. Byrne, and M. Girolami. Langevin diffusions and the metropolis-adjusted langevin algorithm. *Statistics Probability Letters*, 91:14–19, Aug 2014. ISSN 0167-7152. doi: [10.1016/j.spl.2014.04.002](https://doi.org/10.1016/j.spl.2014.04.002). URL <http://dx.doi.org/10.1016/j.spl.2014.04.002>.
- [37] Yale. Linear regression. URL <http://www.stat.yale.edu/Courses/1997-98/101/linreg.htm>.
- [38] Jun Zhu, Jiaming Song, and Bei Chen. Max-margin nonparametric latent feature models for link prediction, 2016.

A Appendix: Additional material

A.1 SBM likelihood and prior

For reference, we provide the likelihoods and priors for the mircocanonical SBM proposed by Peixoto [27]. We have that the graph A is drawn from the SBM:

$$A \sim \text{DC-SBM}_{\text{MC}}(b, e, k) \quad (30)$$

With edges placed uniformly at random but respecting the constraints imposed by b, e and k . The likelihood calculation for $p(A|k, e, b)$ then reduces to a case of counting configurations that yield the same adjacency matrix, $\Xi(A)$, and dividing by the total number of configurations possible, $\Omega(e)$. This is why this formulation is given the microcanonical moniker. If we consider the half-edges to be distinguishable for a moment, the total number of configurations that satisfy the e constraint is:

$$\Omega(e) = \frac{\prod_r e_r!}{\prod_{r,s:r < s} e_{rs}! \cdot \prod_r e_{rr}!!} \quad (31)$$

Where $e_r := \sum_s e_{rs}$ and $(2m)!! := 2^m m!$. Nevertheless, a great number of these configurations yield the same graph A . We denote the number of configurations that yield the adjacency matrix A with $\Xi(A)$, which can be computed as:

$$\Xi(A) := \frac{\prod_i k_i!}{\prod_{i,j : i < j} A_{ij}! \prod_i A_{ii}!!} \quad (32)$$

Note the similarity between the forms of $\Omega(e)$ and $\Xi(A)$ as e is effectively the adjacency matrix of the block-graph. With these defined we can write the overall likelihood:

$$p(A|k, e, b) = \frac{\Xi(A)}{\Omega(e)} \quad (33)$$

Obviously, this form is only defined if A respects the constraints imposed by (k, e, b) else the likelihood is 0. With the likelihood defined, we move on to the prior. As discussed in the main text, for the FFBM b is an intermediate variable and not a parameter so we are not free to choose a prior for it. Nevertheless, we can borrow the conditional prior proposed by Peixoto [27] for $p(e, k|b)$:

$$p(e, k|b) = p(e|b)p(k|e, b) = \left[\begin{Bmatrix} \{ \frac{B}{2} \} \\ E \end{Bmatrix} \right]^{-1} \cdot \left[\prod_r \frac{\prod_j \eta_j^r!}{n_r! q(e_r, n_r)} \right] \quad (34)$$

Where $\{n\}$ is shorthand for $\binom{n+m-1}{m} = \frac{(n+m-1)!}{(n-1)!(m)!}$ which can be thought of as the total number of distinct histograms with n bins under the constraint they sum to m . $E = \frac{1}{2} \sum_{r,s} e_{rs}$ is the total number of edges in the graph. Importantly, E is not allowed to vary and so $p(e|b)$ is uniform with respect to e . The variable η_j^r is introduced to denote the number of vertices in block r that have degree j . Formally, $\eta_j^r := \sum_i \mathbb{1}\{b_i = r\} \mathbb{1}\{k_i = j\}$. Furthermore, $q(m, n)$ is the number of different histograms with at most n non-zero bins that sum to m . $q(m, n)$ is related to but different from $\{n\}$. Recall that $e_r := \sum_s e_{rs}$ is the total number of half edges in block r and $n_r := \sum_i \mathbb{1}\{b_i = r\}$ is the number of vertices assigned to block r .

The form of these priors were chosen carefully by Peixoto [27] to more closely match the structure of empirical networks than simple uniform priors. We do not repeat his arguments here.

A.2 Choosing the MALA step-size

For sampling from the θ -chain of the block membership generator parameters, we employed the Metropolis Adjusted Langevin Algorithm (MALA). At iteration t , the proposed sample is generated by:

$$\theta' = \theta^{(t)} - h_t \nabla U(\theta^{(t)}) + \sqrt{2h_t} \cdot \xi \quad (35)$$

There are two competing objectives when choosing the step-size h_t . On the one hand, we want the step-size to be large so that we arrive at a high density region quickly. However, too large a step-size will lead to a lower acceptance ratio and thus inefficient sampling. A solution to this problem would be to slowly decrease the step-size with t - often called simulated annealing. Therefore, we still have a short burn-in time but will not bounce around the mode for large t . As well as the trivial constraint for h_t to be strictly positive, we introduce two further constraints as outlined by Welling and Teh [35]:

$$\sum_{t=1}^{\infty} h_t = \infty \quad \text{and} \quad \sum_{t=1}^{\infty} h_t^2 < \infty \quad (36)$$

The first constraint ensures that we have cover sufficient distance to arrive at any arbitrary point in our domain, no matter the starting point. The second constraint ensures that once we converge to the mode rather than simply bouncing around it. Welling and Teh [35] propose the following form for a polynomially decaying step-size which we adopt:

$$h_t = \alpha(\beta + t)^{-\gamma} \quad (37)$$

Where α, β, γ are hyper-parameters to be chosen. We require $\alpha, \beta > 0$ and $\gamma \in (0.5, 1]$ to satisfy equation 36. To reduce the number of hyperparameters we set these to have values given by the equations 38.

$$\alpha = \frac{250 \cdot s}{N} \quad \beta = 1000 \quad \gamma = 0.8 \quad (38)$$

Where N is the number of data-points we are considering and now s is the only free variable which we call the step-size scaling. For approximate methods, we can choose to bypass the MH accept-reject entirely to speed up computation. If this is done, the algorithm is instead called stochastic gradient Langevin diffusion (SGLD) [35]. This speeds up computation at the expense of exactness of the method.

Nevertheless, to choose the value of s we must quantify the trade-off between acceptance ratio and burn-in time. We do this by way of an example with the primary school dataset [33]. We run the b -chain for $T_b = 1,000$ iterations and subsample such that \mathcal{T}_b is computed with $\kappa_b = 0.2$ and $\lambda_b = 5$. We then use this to run the θ -chain for $T_\theta = 10,000$ iterations. The acceptance ratio – which we denote r_α – is easy enough to compute as simply the fraction of proposed moves which we accept. However, to quantify burn-in time we must use a different metric. We can plot the mean of the objective function averaged over all samples as a proxy for burn-in time:

$$\bar{U} := \frac{1}{T_\theta} \sum_{t \in [T_\theta]} U(\theta^{(t)}) \quad (39)$$

As the chain will equilibrate in the vicinity of a minima in $U(\theta)$, the average over all samples is a rough indicator of the speed of burn-in. This assumes that the random starting point has high $U(\theta)$. The higher the value of \bar{U} , the longer the chain took to burn in and reach equilibrium. We plot the acceptance ratio r_α and average objective \bar{U} for 10 values of the step-size multiplier s logarithmically spaced in the range $(10^{-2}, 10^1)$ on figure 5.

We see immediately that acceptance ratio r_α steadily decreases with s . This is expected as it is unlikely we stay in a high density region of our target distribution if we are making very large steps each time. A low acceptance ratio leads to wasted samples and this inefficiency is obviously undesirable. Nevertheless, \bar{U} decreases with s indicating shorter burn-in times for larger step-sizes. Nevertheless, this effect plateaus for $s > 0.2$ for this particular dataset. Therefore, we choose $s = 0.2$ as our step-size multiplier for the primary school datasets as this yields the best trade-off between r_α and \bar{U} . Indeed, the acceptance ratio is still high for $r_\alpha \approx 0.8$ for $s = 0.2$. The step-sizes for the other datasets were chosen following the same argument.

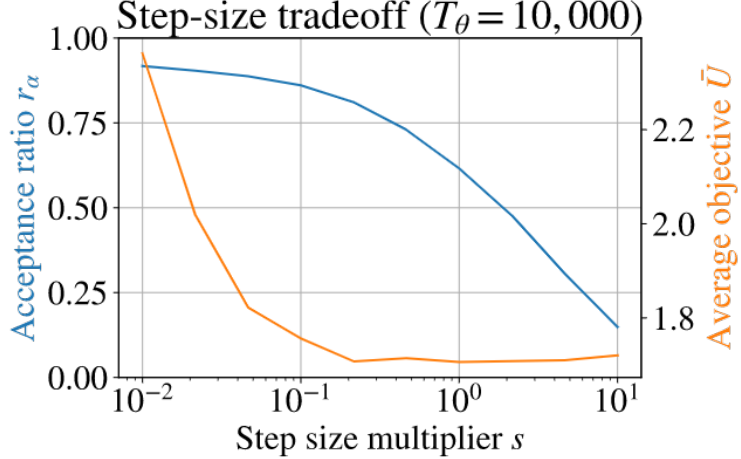


Figure 5: Primary school dataset [33] illustration of step-size tradeoff

A.3 Burn-in and thinning

As with any MCMC method, we must deal with the issues presented by burn-in and thinning. We have introduced the notation \mathcal{T}_b and \mathcal{T}_θ to denote the set of samples we keep from the b and θ chains respectively. Note that we generate T_b and T_θ samples total. The burn-in period refers to the time taken for the Markov Chain to converge to the stationary distribution. Sample thinning is necessary to ensure that neighbouring samples satisfy independence. However, as we do not leverage the independence property this is less important in our analysis. We can write the general set \mathcal{T}_* as:

$$\mathcal{T}_* = \{T_* \kappa_* + i \lambda_* : 0 \leq i \leq [T_*(1 - \kappa_*)/\lambda_*]\} \quad (40)$$

Where the parameter $\kappa_* \in (0, 1)$ controls our burn-in and λ_* controls our thinning. κ_* can be determined by plotting the log-target (either $S(b^{(t)})$ or $U(\theta^{(t)})$) with respect to the epoch t . κ_* is then chosen to encompass the region where the log-target has roughly equilibrated. As we do not leverage sample independence λ_* can be chosen less rigorously. We often just use $\lambda_b = 5$ and $\lambda_\theta = 10$.

By way of illustration, we can consider the primary school dataset [33]. We plot the normalised objective function $U(\theta^{(t)})/N$ with respect to MALA iteration on figure 6a. We see that the chain converges to the modal neighbourhood quickly (within about 2000 iterations of a total 10,000). Nevertheless, we pick $\kappa_\theta = 0.4 > 0.2$ just to be on the safe-side. $\lambda_\theta = 10$ is chosen somewhat arbitrarily as we do not require neighbouring samples to be independent. Nevertheless, this thinning does speed up computation of quantities that require an average over all the retained samples – as $|\mathcal{T}_\theta| < T_\theta$.

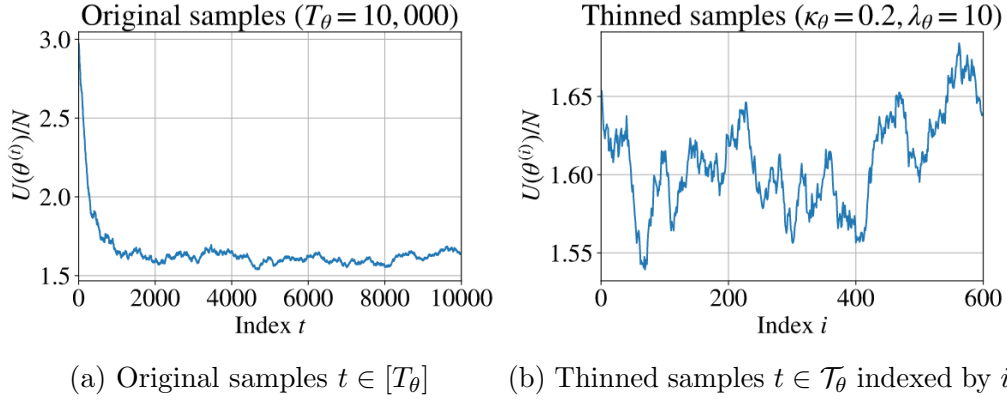


Figure 6: Primary school dataset normalised objective function against sample index

We see on figure 6b that $U(\theta^{(i)})$ does bounce around a small amount. This is to be expected we are sampling from the posterior rather than converging to the MAP. The variations do appear to be rather long in time-scale but we can live with this as we do not require sample independence.

A.4 Initializing the b-chain

For the purposes of our model (the FFBM), the number of blocks B is a constant which must be specified by the data scientist. We could however, allow our choice of B to be influenced by the observed data. This places us in the domain of empirical Bayes, which must be negotiated carefully. Prior beliefs must be determined a priori else they are not prior. However, as the number of blocks only specifies the coarseness of the analysis, it is fine to allow it to vary. Indeed, Peixoto [24] shows that for a fixed average degree the maximum number of detectable blocks scales as $O(\sqrt{N})$ where N is the number of vertices.

If we allow B to vary in the b -chain (i.e. new blocks can be created and we permit empty blocks) then it can be run until a minimum description length (MDL) solution is reached. We take the number of non-empty blocks at the MDL to be our fixed block number B for subsequent analysis. Indeed, it is prudent to start our b -chain at this MDL solution as then we can burn-in time is greatly reduced.

A.5 Dimensionality discussion

There is a challenge when dealing with vertex-features. Many vertex feature often take only one of several discrete values within a set. For example, with the primary school dataset [33], a pupil's school-class can take one of 10 values from {"1A", "1B", "2A", "2B" ... "5A", "5B"}.

It is not immediately obvious how to encode this for the feature-to-block classifier. Although this is technically only a single dimension, we choose to expand the data into a set of 10 binary feature flags $\in \mathcal{X} = \{0, 1\}$. Although only one flag will be set at a time it is the simplest method for representing discrete-valued data. The reason we choose $\mathcal{X} = \{0, 1\}$ and not $\mathcal{X} = \{-1, 1\}$ is that the former allows for simpler analysis of the resulting weight values. When a feature is switched off, it has no impact on the softmax classifier. It is simpler to only model positive relationships. We prefer to say that this block is comprised of the vertices with feature d on rather than this block contains the vertices with feature d switched off. To make this explicit, say we have a feature encoding a pupil's gender: {"male", "female"}, we represent this as 2 binary feature flags "male": {0, 1} and "female": {0, 1}. This approach may seem inefficient but it is vital to ensure we can interpret the resulting parameter distributions.

Nevertheless, this dimensionality expansion means that we cannot include a bias term in our classifier as then the MAP solution is less peaked and our θ -samples will have higher variance. To illustrate this point we need only look at the form of the soft-max classifier with bias vector β , operating on a vector x which only has feature d turned on such that $x_i = \mathbb{1}\{i = d\}$. Component j of the output is given by:

$$\phi_j(x) = \frac{\exp(w_j^T x + \beta_j)}{\sum_{k=1}^B \exp(w_k^T x + \beta_k)} = \frac{\exp(w_{jd} + \beta_j)}{\sum_{k=1}^B \exp(w_{kd} + \beta_k)} \quad (41)$$

For the case that x can only has one entry $x_d = 1$ and the rest are 0, the term $w_{kd} + \beta_k$ is effectively the new weight for component k . The bias term β_k becomes an unnecessary extra degree of freedom. To illustrate this point, we set $\beta_k = \beta_0 \forall j$. If this is the case then equation 41 can be simplified to:

$$\phi_j(x) = \frac{\exp(\beta_0) \cdot \exp(w_{jd})}{\sum_{k=1}^B \exp(\beta_0) \cdot \exp(w_{kd})} = \frac{\exp(w_{jd})}{\sum_{k=1}^B \exp(w_{kd})} \quad (42)$$

This expression is independent of β_0 and so it is free to vary. This is not the whole picture as we also have the prior which introduces a regularisation term which favours weights closer to 0. Nevertheless, for mutually exclusive binary feature flags, the bias term does not add to the expressiveness of the model and only serves to complicate analysis. We therefore remove the bias term from the Softmax classifier. Even for data comprised of several such features (e.g. school class and data) we prefer to discard the bias term. The bias term only serves to decrease the loss function by leveraging information about the size of each detected block and not feature information. We do not wish to be overly confident in our model predictions when such prediction is influenced by block size and not feature information. Indeed, the

approach was initially developed with a bias term but we found its removal yielded more reliable and reproducible results.

B Appendix: Derivations

B.1 Derivation of conditional block distribution given feature matrix

We wish to determine the form of $p(b|X)$. This can be done by integrating over the joint probability with respect to θ .

$$\begin{aligned} p(b|X) &= \int p(b, \theta|X, \theta)d\theta = \int p(b|X, \theta)p(\theta|X)d\theta \\ &= \int p(b|X, \theta)p(\theta)d\theta = \int \prod_{i \in [N]} \phi_{b_i}(x_i; \theta)p(\theta)d\theta \\ &= \prod_{i \in [N]} \int \frac{\exp(w_{b_i}^T \tilde{x}_i) \prod_{j \in [B]} \mathcal{N}(w_j; 0, \sigma_\theta^2 I)}{\sum_{k \in [B]} \exp(w_k^T \tilde{x}_i)} dw_{1:B} \end{aligned}$$

We note that $b_i \in [B]$ and so the integral's value is unchanged with respect to b_i . The integrand has the same form no matter which value b_i takes as the prior is the same for each w_j . As such the integral can only be a function of at most \tilde{x}_i and σ_θ^2 as it is symmetric with respect to b_i and all the various w_j are integrated out as they are dummy variables. Therefore, denoting the integral by the (unknown) function $f(\tilde{x}_i, \sigma_\theta^2)$, we write $p(b|X)$ as follows:

$$p(b|X) = \prod_{i=1}^N f(\tilde{x}_i, \sigma_\theta^2) = \text{const w.r.t } b = c$$

As this is a constant with respect to b we conclude that $p(b|X)$ must be a uniform distribution. $1/c$ is simply the size of the set of values that b can take. We know $b_i \in [B]$. Therefore, $b \in [B]^N$ and $|[B]^N| = B^N = 1/c$. Putting this all together we conclude that:

$$p(b|X) = B^{-N} \tag{43}$$

B.2 Derivation of U form

The invariant distribution we wish to target for the θ samples is the posterior of θ given the values of the pair (X, b) . We write this as follows:

$$\pi_\theta(\theta) \propto p(\theta|X, b) \propto p(b|X, \theta)p(\theta) \propto \exp(-U(\theta)) \tag{44}$$

$$\therefore U(\theta) = -(\log p(b|X, \theta) + \log p(\theta)) + \text{const} \tag{45}$$

Where we have introduced $U(\theta)$ equal to the negative log posterior. Each of the constituent terms of $U(\theta)$ are easily computed (equation 46) by defining $y_{ij} := \mathbb{1}\{b_i = j\}$ and $a_{ij} := \phi_j(x_i; \theta)$.

$$\log p(b|X, \theta) = \sum_{i \in [N]} \sum_{j \in [B]} y_{ij} \log a_{ij} \quad \text{and} \quad \log p(\theta) = -\frac{(D+1)(B)}{2} \log 2\pi - \frac{1}{2\sigma_\theta^2} \|\theta\|^2 \quad (46)$$

Discarding constant terms, we write $U(\theta)$ as in equation 47. Note that $\|\theta\|^2 = \sum_i \theta_i^2 = \sum_{j=1}^B \|w_j\|^2$ is the Euclidean norm of the vector of parameters θ .

$$U(\theta) = \left(\sum_{i=1}^N \sum_{j=1}^B y_{ij} \log \frac{1}{a_{ij}} \right) + \frac{1}{2\sigma_\theta^2} \|\theta\|^2 = N \cdot \mathcal{L}(\theta) + \frac{1}{2\sigma_\theta^2} \|\theta\|^2 \quad (47)$$

B.3 Derivation of U gradient with respect to feature parameters

The goal is to determine $\nabla U(\theta)$, the gradient of the negative log posterior with respect to the parameters. We repeat the form of $U(\theta)$ in equation 48.

$$U(\theta) = \left(\sum_{i \in [N]} \sum_{j \in [B]} y_{ij} \log \frac{1}{a_{ij}} \right) + \frac{1}{2\sigma_\theta^2} \|\theta\|^2 \quad (48)$$

Where y_{ij} is independent of θ and a_{ij} is the output from the softmax layer, with form as given in equation 49.

$$a_{ij} := \phi_j(x_i; \theta) = \frac{\exp(w_j^T \tilde{x}_i)}{\sum_{r \in [B]} \exp(w_r^T \tilde{x}_i)} \quad (49)$$

We note that $\theta = \{w_k\}_{k=1}^B$, and as such we can write this in vector form $\theta = [w_1^T, w_2^T \dots w_B^T]^T$. Therefore, $\nabla U(\theta) = [\partial U / \partial w_1^T, \partial U / \partial w_2^T \dots \partial U / \partial w_B^T]^T$; to compute $\nabla U(\theta)$ it suffices to find the form of $\partial U / \partial w_k$ with respect to a general k .

To this end, we must first find partial derivatives of a_{ij} and $\|\theta\|$ with respect to w_k . Starting with a_{ij} :

$$\begin{aligned} \frac{\partial a_{ij}}{\partial w_k} &= \frac{\tilde{x}_i \exp(w_j^T \tilde{x}_i) \delta_{jk} \cdot \sum_{r \in [B]} \exp(w_r^T \tilde{x}_i) - \exp(w_j^T \tilde{x}_i) \cdot \tilde{x}_i \exp(w_k^T \tilde{x}_i)}{\left(\sum_{r \in [B]} \exp(w_r^T \tilde{x}_i) \right)^2} \\ &= \tilde{x}_i (a_{ij} \delta_{jk} - a_{ij} a_{ik}) \end{aligned} \quad (50)$$

Where $\delta_{jk} := \mathbb{1}\{j = k\}$. Now moving onto the derivative of $\|\theta\|^2$:

$$\frac{\partial}{\partial w_k} \|\theta\|^2 = \frac{\partial}{\partial w_k} \left(\sum_{r \in [B]} \|w_r\|^2 \right) = 2w_k \quad (51)$$

We are ready to put this all together, to find the partial derivative of $U(\theta)$ with respect to each w_k :

$$\begin{aligned} \frac{\partial U}{\partial w_k} &= \sum_{i=1}^N \sum_{j=1}^B y_{ij} \left(\frac{-\tilde{x}_i}{a_{ij}} (a_{ij}\delta_{jk} - a_{ij}a_{ik}) \right) + \frac{w_k}{\sigma_\theta^2} \\ &= - \left(\sum_{i=1}^N \tilde{x}_i \left(y_{ik} - a_{ik} \sum_{j=1}^B y_{ij} \right) - \frac{w_k}{\sigma_\theta^2} \right) \\ &= - \left(\sum_{i=1}^N \left\{ \tilde{x}_i (y_{ik} - a_{ik}) \right\} - \frac{w_k}{\sigma_\theta^2} \right) \end{aligned} \quad (52)$$

This is the required result. This form can be computed efficiently through matrix operations. The only property of y_{ij} we have used in the derivation is the sum-to-one constraint $\sum_{j=1}^B y_{ij} = 1$ for all i .

C Appendix: Implementation details

C.1 Algorithms

Algorithm 1 Block membership sample generation

```
procedure SAMPLEBLOCKMEMBERSHIPS( $A, T_b$ )
     $b^{(0)} \leftarrow \arg \min_b S(b|A)$             $\triangleright$  Implemented as greedy heuristic in graph-tool library
    for  $t \in \{0, 1 \dots T_b - 1\}$  do
         $b' \leftarrow \sim q_b(b^{(t)}, b'|A)$ 
         $\log \alpha_b \leftarrow \log \alpha_b(b^{(t)}, b'|A)$ 
         $\eta \leftarrow \sim \text{Unif}(0, 1)$ 
        if  $\log \eta < \log \alpha_b$  then
             $b^{(t+1)} \leftarrow b'$ 
        else
             $b^{(t+1)} \leftarrow b^{(t)}$ 
        end if
    end for
    return  $\{b^{(t)}\}_{t=1}^{T_b}$ 
end procedure
```

Algorithm 2 FFBM parameter pseudo-marginal inference

```
procedure SAMPLEFEATUREWEIGHTS( $X, \{b^{(t)}\}, \mathcal{T}_b, \sigma_\theta, s$ )
     $\hat{Y}_{ij} \leftarrow \frac{1}{|\mathcal{T}_b|} \sum_{t \in \mathcal{T}_b} \mathbb{1}\{b_i^{(t)} = j\} \quad \forall i, j$ 
     $\theta^{(0)} \leftarrow \sim \mathcal{N}(0, \sigma_\theta I)$ 

    for  $t \in \{0, 1 \dots T_\theta - 1\}$  do
         $\xi \leftarrow \sim \mathcal{N}(0, I)$ 
         $h_t \leftarrow \frac{s}{N} \cdot 250(1000 + t)^{-0.8}$ 
         $g_t \leftarrow \nabla U(\theta^{(t)} | X, \hat{Y})$ 

         $\theta' \leftarrow \theta^{(t)} - h_t \cdot g_t + \sqrt{2h_t} \cdot \xi$ 
         $\log \alpha_\theta \leftarrow \log \alpha_\theta(\theta^{(t)}, \theta' | A, \hat{Y})$ 
         $\eta \leftarrow \sim \text{Unif}(0, 1)$ 
        if  $\log \eta < \log \alpha_\theta$  then
             $\theta^{(t+1)} \leftarrow \theta'$ 
        else
             $\theta^{(t+1)} \leftarrow \theta^{(t)}$ 
        end if
    end for
    return  $\{\theta^{(t)}\}_{t=1}^{T_\theta}$ 
end procedure
```

Algorithm 3 Dimensionality reduction

```
procedure REDUCEDIMENSION( $\{W^{(t)}\}, \mathcal{T}_\theta, k, D'$ )
     $(B, D) \leftarrow W^{(0)}$ .shape
     $\hat{\mu}_{ij} \leftarrow \frac{1}{|\mathcal{T}_\theta|} \sum_{t \in \mathcal{T}_\theta} W_{ij}^{(t)} \quad \forall i \in [B], j \in [D]$ 
     $\hat{\sigma}_{ij} \leftarrow \frac{1}{|\mathcal{T}_\theta|} \sum_{t \in \mathcal{T}_\theta} \left( W_{ij}^{(t)} - \hat{\mu}_{ij} \right)^2 \quad \forall i \in [B], j \in [D]$ 

    for  $d \in [D]$  do
        for  $i \in [B]$  do
             $l_i \leftarrow \hat{\mu}_{id} - k \cdot \hat{\sigma}_{id}$ 
             $u_i \leftarrow \hat{\mu}_{id} + k \cdot \hat{\sigma}_{id}$ 
            if  $l_i \leq 0$  and  $u_i \geq 0$  then
                 $l_i, u_i \leftarrow 0$ 
            end if
        end for
         $c_d \leftarrow \max_i \min(|l_i|, |u_i|)$ 
    end for

    indexArray  $\leftarrow$  indexSort( $c$ , descending=True)[ $0 : D'$ ]
     $d^* \leftarrow$  indexArray[-1]
     $\mathcal{D}' \leftarrow$  Set(indexArray)
     $c^* \leftarrow c_{d^*}$ 
    return  $\mathcal{D}', c^*$ 
end procedure
```

C.2 Hyperparameter values

Table 3: Hyper-parameter values for each experiment

Dataset	B	f	σ_θ	T_b	κ_b	λ_b	T_θ	κ_θ	λ_θ	s	k	D'	T'_θ	κ'_θ	λ'_θ	s'
Polbooks	3	0.7	1	1,000	0.2	5	10,000	0.4	10	0.05	—	—	—	—	—	—
School	10	0.7	1	1,000	0.2	5	10,000	0.4	10	0.2	1	10	10,000	0.4	10	0.2
FB Egonet	10	0.7	1	1,000	0.2	5	10,000	0.4	10	0.017	1	10	10,000	0.4	10	0.5

C.3 Hardware specification

All data analysis and visualisation was implemented in Python. Full source code is available in the supplementary material. The scripts were run using a standard PC using the Windows Subsystem for Linux (WSL) environment. Specs are:

- **CPU:** Intel(R) Core(TM) i7-1065G7
- **RAM:** 8GB
- **GPU:** Intel(R) Iris(R) Plus Graphics

On this hardware each experiment iteration took the following amount of time to execute:

Table 4: Compute-time for each experiment

Dataset	b -chain	θ -chain	Reduced θ -chain	Overall compute time
Polbooks	~1s	~10s	—	~11s
School	~1s	~7s	~7s	~15s
FB Egonet	~2s	~50s	~8s	~60s

D Risk assessment retrospective

As experimental work was entirely computer-based the risks encountered were not what one might typically associate with a more hands-on project: heavy machinery, dangerous chemicals etc. Most of the risks identified would be as a result of an improper working environment. These could be properly managed by ensuring the working environment felt comfortable. An external monitor went some way to alleviating the eye-strain of coding on a small screen for extended periods. Furthermore, an external mouse is far kinder on the wrist than a track-pad on laptops. There were no unexpected hazards encountered that were not identified at the start of the project.

E Covid-19 disruption

Thankfully this project was not directly disrupted by Covid-19 as it was always going to be heavily theoretical and computational. The only disruption to speak of was the shift of supervisor meetings to online. Though shared whiteboards were alien at first, we grew to learn how to use them to effectively communicate ideas.

I was ill with Covid-19 for 2 weeks in October but this did not majorly impact my ability to work. The Covid-19 contingency plan formulated last summer and documented on the Project Planning Form just involved switching supervisions to an online format.